





# Composite confining systems: Rethinking geologic seals for permanent CO<sub>2</sub> sequestration

[Alexander P. Bump](#)  , [Sahar Bakhshian](#), [Hailun Ni](#), [Susan D. Hovorka](#), [Marianna I. Olariu](#), [Dallas Dunlap](#), [Seyyed A. Hosseini](#), [Timothy A. Meckel](#)

[Show more](#) 

 [Outline](#) |  [Share](#)  [Cite](#)

<https://doi.org/10.1016/j.ijggc.2023.103908> 

[Get rights and content](#) 

Under a Creative Commons [license](#) 

*open access*

## Highlights

- Composite confining systems are multi-layer systems of discontinuous barriers.
- They work by drastically lowering effective  $K_v/K_h$ , creating long flow paths for CO<sub>2</sub>.
- Migration-assisted trapping effectively immobilizes CO<sub>2</sub> with little vertical migration.
- Risks are familiar—legacy wells, permeable faults and high-relief structures.
- Composite confining systems are ideally suited to the goal of permanent sequestration.

## Abstract

Permanent containment is paramount for geologic carbon sequestration. Petroleum experience proves the possibility but also creates bias—to date, carbon storage projects have used seals similar to those of producing petroleum accumulations—thick, laterally extensive, effectively impermeable layers. These work

for CO<sub>2</sub>, but may not be present where needed, nor optimal for sequestration. We introduce the concept of composite confining systems, defined here as multi-layer stratigraphic systems of discontinuous barriers with no a priori requirements for continuity or minimum capillary entry pressure. We explore the concept through physical analog modeling, geologic characterization and full-scale numerical modeling. We find that barriers need only offer enough capillary entry pressure contrast to divert the flow of CO<sub>2</sub> and that barrier frequency and barrier area are the key variables in retarding vertical migration. Data from Southern Louisiana Miocene deltaic deposits shows ~5–15 mudstone barriers/100m of section, with average mudstone lengths of over 1 km and aspect ratios ~2:1, giving effective ratios of vertical to horizontal permeability ( $k_v/k_h$ ) of ~0.0005. Full-scale reservoir models show that these systems can completely arrest vertical migration of industrial-scale volumes of CO<sub>2</sub> (10's of megatons) within a few 10's of meters of stratigraphic section. Unlike more conventional petroleum seals and traps, which retain CO<sub>2</sub> in a concentrated, mobile state, composite confining systems disperse and immobilize it via migration-assisted trapping. The greatest risks to performance of composite confining systems are the same as for conventional seals—the potential shortcuts across stratigraphic barriers, e.g., legacy wells, fluid escape pipes and permeable faults that focus flow.



## Keywords

CCS; Composite confining system; Containment; Seal; Geologic carbon storage; Leakage risk; Confining zone; Migration-assisted trapping; Storage security; Risk; Leakage

## 1. Introduction

In the quest to mitigate climate change, there are many viable reservoirs for sequestering carbon, including biomass, soil, oceans and subsurface geologic reservoirs. All can be effective, but the latter are unique for the timescale of retention that they offer. Whereas biomass, soil and oceans can retain carbon for years to decades or perhaps even centuries, geologic storage operates on a scale of millions to tens or even hundreds of millions of years ([Haszeldine and Scott, 2014](#)). With respect to climate change and human needs, it is effectively permanent. Nevertheless, there are persistent worries among investors and the public about the longevity of retention in saline storage projects and the possible leakage of both injected CO<sub>2</sub> and ambient subsurface brines ([Paluszny et al., 2020](#); [Hart and Schlossberg, 2021](#); [Dermansky, 2023](#); [Mullin, 2023](#)). Those concerns are reflected in public skepticism, academic research focus and regulatory requirements to disprove potential leakage through site characterization, modeling and ongoing monitoring.

Experience with hydrocarbons offers a natural and common starting point for geologic CO<sub>2</sub> sequestration in saline aquifers. Like CO<sub>2</sub>, hydrocarbons are buoyant fluids that migrate generally upward in the subsurface until their progress is blocked by a seal capable of retaining the buoyancy pressure and a trapping geometry that prevents lateral escape. Classically, these seals (or “caprocks”) are discrete, laterally extensive geologic units with uniformly high capillary entry pressure and a sharp contact with the underlying reservoir, such that minimal hydrocarbons are lost in a transitional “waste zone” where waning permeability allows

hydrocarbon invasion but from which, production is uneconomic (Schowalter and Hess, 1982). Common examples of high-quality seals include transgressive marine shales and layered evaporites. Over a century of experience in hydrocarbon exploration and production has proven unequivocally that such seals can retain large columns of buoyant fluids (including naturally occurring CO<sub>2</sub>) for geologic time (Grunau, 1987; Downey, 1994; Lu et al., 2009; IEAGHG, 2011; Miocic et al., 2016; Kampman et al., 2016).

Concerns about retention in geologic carbon storage (GCS) have naturally prompted developers to focus on similarly high-quality seals for GCS. Indeed, most GCS projects to date have followed that model, sometimes even employing multiple redundant regional seals for added insurance (e.g., Quest; IEAGHG 2019). That approach is effective. However, the analog of hydrocarbon fields is predicated on the need to produce fluids, i.e., the need to find large, concentrated volumes of mobile hydrocarbons that can be recovered economically. GCS, on the other hand, has a different set of goals and constraints. GCS seeks to inject CO<sub>2</sub> on multi-decadal timescales with retention for millennia. Most importantly, the goal of GCS is permanent sequestration, not recovery. Together, these differences suggest reevaluating our ideas on the geologic requirements for secure CO<sub>2</sub> containment.

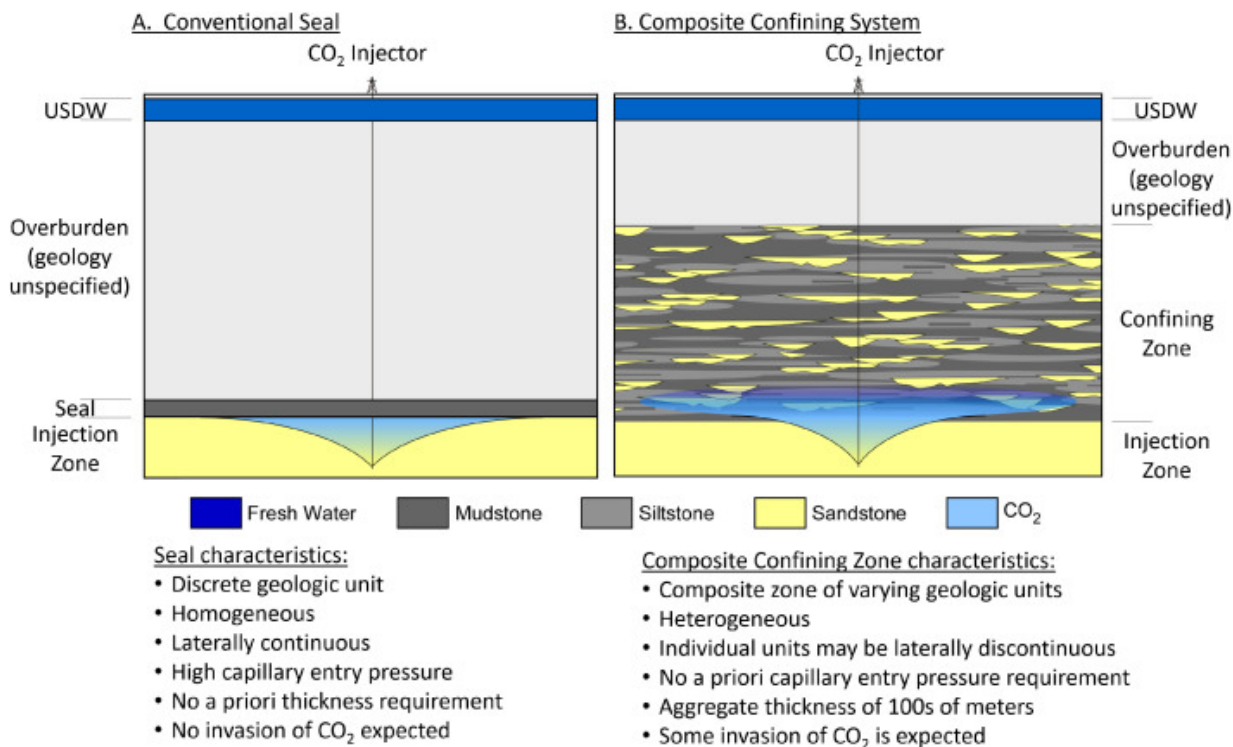
The regulations for GCS are not prescriptive with respect to geologic seals. The US EPA, for example, requires only “confining zone(s) free of transmissive faults or fractures and of sufficient areal extent and integrity to contain the injected carbon dioxide stream and displaced formation fluids and allow injection at proposed maximum pressures and volumes without initiating or propagating fractures in the confining zone(s)” (UIC Class VI, 2010). The EU CCS Directive states that “a geological formation shall only be selected as a storage site, if under the proposed conditions of use there is no significant risk of leakage, and if no significant environmental or health risks exist.” In detail, it skews only slightly closer to classic petroleum seals than Class VI, specifying that “dynamic modeling shall provide insight into... CO<sub>2</sub> trapping mechanisms and rates (including spill points and lateral and vertical seals); secondary containment systems in the overall storage complex; ...[and] the risk of CO<sub>2</sub> entry into the caprock.” The definition of “caprock” is never specified and is as close as the directive comes to requiring a single seal (Directive 2009/31/EC, 2009). ISO 27914:2017(E) is the most specific of the major standards, describing characterization of a “primary seal.” However, it too acknowledges the use of “secondary barriers to CO<sub>2</sub> leakage,” including “permeable strata and secondary seals,” both above and within the storage complex (ISO/TC 265, 2017). In sum, there is clear agreement that containment is paramount, but also considerable freedom to define how that is achieved.

The purpose of this paper is to define and explore the effectiveness of a new concept of confining system, reimagined for the goal of permanent sequestration with no intention of future recovery. We focus here on containment with respect to vertical migration, although similar concepts could be applied to containing lateral flow.

## 2. Composite confining systems

We define a composite confining system as a multi-layer stratigraphic system of sub-horizontal but potentially discontinuous flow barriers with no a priori requirement for minimum capillary entry pressure values or lateral continuity of individual elements (Fig. 1). Barriers need only present sufficient resistance to vertical flow to divert migrating CO<sub>2</sub> and displaced brines and they need only be distributed such that the gaps between the barriers are not all in vertical alignment. In engineering terms, composite confinement

systems work by lowering the ratio of effective vertical to horizontal permeability ( $k_v/k_h$ ) for a given thickness of stratigraphy. The presence of horizontal barriers diverts vertical flow, creating a long, tortuous path that spreads migrating fluids laterally, reduces the driving force (column height) and attenuates the mobile fraction through dissolution, residual trapping and local buoyant traps (also known as buoyancy traps). In concept these buoyant traps might range in size from centimeter-scale cross-beds to meter-scale ripples on flow unit tops to small anticlines and stratigraphic pinch-outs, each of which retains a small amount of CO<sub>2</sub> (e.g., [Gasda et al. 2013](#)). For all of these mechanisms, the local quantities of trapped CO<sub>2</sub> are low relative to a single buoyant trap such as a depleted field. The net result of this dispersion is to minimize the potential for unintended migration of CO<sub>2</sub> from the storage complex through any single path.



[Download : Download high-res image \(632KB\)](#)

[Download : Download full-size image](#)

Fig. 1. Schematic diagram illustrating the similarities and differences between conventional seals (A) and composite confining zones (B). “USDW” refers to Underground Source of Drinking Water, i.e., a protected aquifer.

While unfamiliar in this context, the concept of composite confinement builds on well-established principles and proven analogs. In the broadest sense, the idea that a composite system of individually imperfect barriers can create highly effective confinement is encapsulated by Reason's “Swiss cheese model” of accident prevention, which is applied to everything from internet security to aviation safety, Covid-19 containment, and even wartime defense ([Reason, 2000](#); [Shappell and Wiegmann, 2000](#); [Tanimoto et al., 2020](#); [Roberts, 2020](#); [Spencer and Collins, 2022](#)). In terms of subsurface fluid flow, a long series of hydrologic experiments and numerical models has shown that inclusion of even minor, discontinuous permeability barriers could slow or stop the convective mixing of variable density fluids, including dissolved CO<sub>2</sub> ([Schincariol and Schwartz, 1990](#); [Vithanage et al., 2012](#); [Agartan et al., 2015, 2017](#)). [Agartan et al.](#)

(2015, 2017) also noted that low-permeability layers also trapped dissolved CO<sub>2</sub> on their upper surfaces and within the layers themselves, further reducing mobility.

Indeed, the elements of composite confining systems have even been discussed in the literature on CO<sub>2</sub> sequestration. As far back as 1996, the Joule II report showed upward migration of supercritical CO<sub>2</sub> retarded by layered reservoirs (Holloway, 1996). Lindberg modeled the distribution of CO<sub>2</sub> in an aquifer with layered heterogeneities and found that it effectively attenuated vertical migration even without a robust top seal (Lindeberg, 1997). Nordbotten et al. (2009) showed that even with a leak in the primary seal, overlying low-permeability layers could divert vertical migration and retain significant volumes of CO<sub>2</sub>. Oldenburg discussed the use of secondary and tertiary seals (Oldenburg and Unger, 2003; Oldenburg, 2008) and Green and Ennis-King explored break-through times and residual trapping in composite systems with short barriers to support development of the Southwest Hub (Green and Ennis-King, 2010, 2013, 2015; Sharma et al., 2017). What is new here is (1) the explicit recognition that composite confinement is not simply insurance for retention by a conventional seal, but highly effective containment in its own right; (2) that it is ideally suited to the goal of permanent sequestration; and (3) the definition of “retention capacity” as the amount of CO<sub>2</sub> that can be safely stored.

### 3. Exploring the concept

Begget al. (1985) presented a simple model, considering Darcy flow in a layered reservoir with randomly distributed, discontinuous horizontal barriers:

$$K_{VE} = \frac{N:G}{(1+f\bar{d})\left(\frac{1}{k_v} + \frac{f}{k_h}\bar{d}\right)} \quad (1)$$

where  $K_{VE}$  is the effective vertical permeability,  $N : G$  is the net:gross ratio of the reservoir,  $f$  is the number of barriers per meter,  $\bar{d}$  is the average horizontal flow path extension and  $k_v$  and  $k_h$  are the vertical and horizontal permeabilities of the sand, respectively. For the purpose of this calculation, a “barrier” is defined as any permeability contrast capable of diverting flow of the fluid of interest. In three dimensions, the average flow path extension  $\bar{d}$  is defined by the average lateral dimensions of the barriers:

$$\bar{d} = \frac{\bar{w}}{6\bar{l}}(3\bar{l} - \bar{w}) \quad (2)$$

where  $\bar{w}$  and  $\bar{l}$  are the average width and length of the barriers, respectively. It can be seen from Eq.(1) that effective vertical permeability is inversely proportional to the squares of barrier frequency and average lateral dimensions and directly proportional to net:gross. However, the equation also prompts questions: What constitutes a barrier? What is their actual frequency in the subsurface and how do we define their average lateral extent? And of course, how does effective vertical permeability translate to retention of CO<sub>2</sub>? We investigate these questions in the following sections. Given our interest in arresting vertical migration, we focus on stratigraphic barriers. However, low-angle structural features such as faults, deformation bands and stylolites could also provide effective barriers, at least in principle.

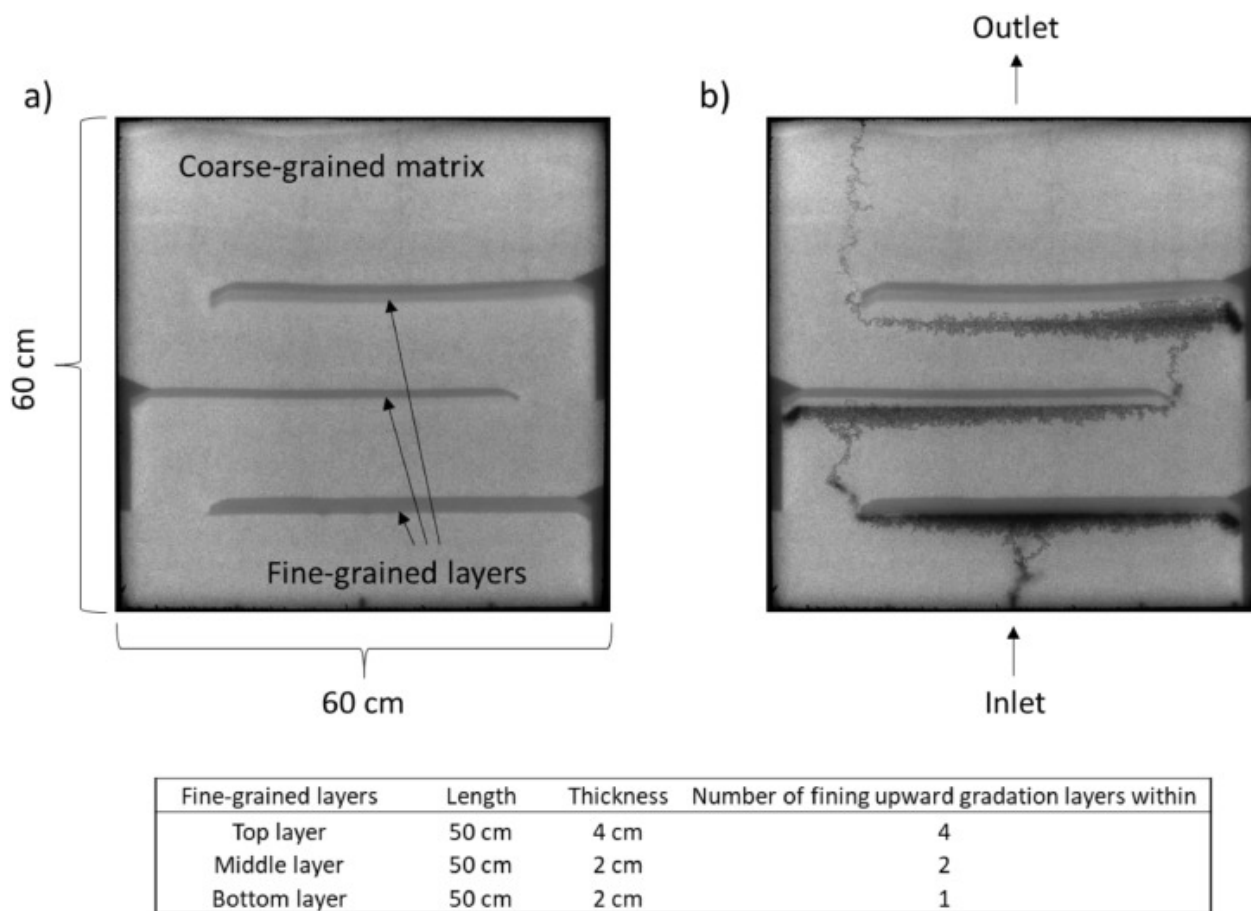
### 4. Physical analog modeling

To investigate the ability of barriers to divert flow, we conducted physical fluid flow experiments, using tank-scale bead packs (Fig.2). In the experiment shown in Fig.2a, the tank contains three fine-grained layers

of equal length but with variable thickness and variable numbers of subsidiary layers that fine upward. The fine-grained layers are all open at one end and sealed at the other end with even finer grains. The sealed end is therefore closed to fluid flow. The glass bead grain sizes used for the coarse-grained matrix and the finest (topmost) layers have mean diameters of 0.689 mm and 0.331 mm, respectively—equivalent to coarse and medium sand (Wentworth, 1922; Krishnamurthy, 2020). The capillary entry pressure contrast between the matrix (216 Pa) and the finest (topmost) layer (477 Pa) is 0.45. Using the Leverett J-function scaling equation (Leverett, 1941),

$$\frac{k_v}{k_h} = \left( \frac{P_{c,h}}{P_{c,v}} \right)^2 \quad (3)$$

where  $P_{c,h}$  and  $P_{c,v}$  are the capillary entry pressure values of the matrix and the finest layer respectively, we can compute the equivalent  $k_v/k_h$  ratio from the capillary entry pressure ratio, and it is about 0.2. This calculation assumes that porosity, interfacial tension, and contact angle values are all constant. The intermediate gradational layers lie between these endmembers in both grain size and capillary entry pressure.



[Download : Download high-res image \(628KB\)](#)

[Download : Download full-size image](#)

Fig. 2. Physical tank-scale beadpack fluid flow experimental results. (a) Image of the beadpack filled with the wetting phase fluid taken before injection began. (b) Image of the beadpack at the end of the drainage experiment at domain percolation; the nonwetting phase plume is shown in black.

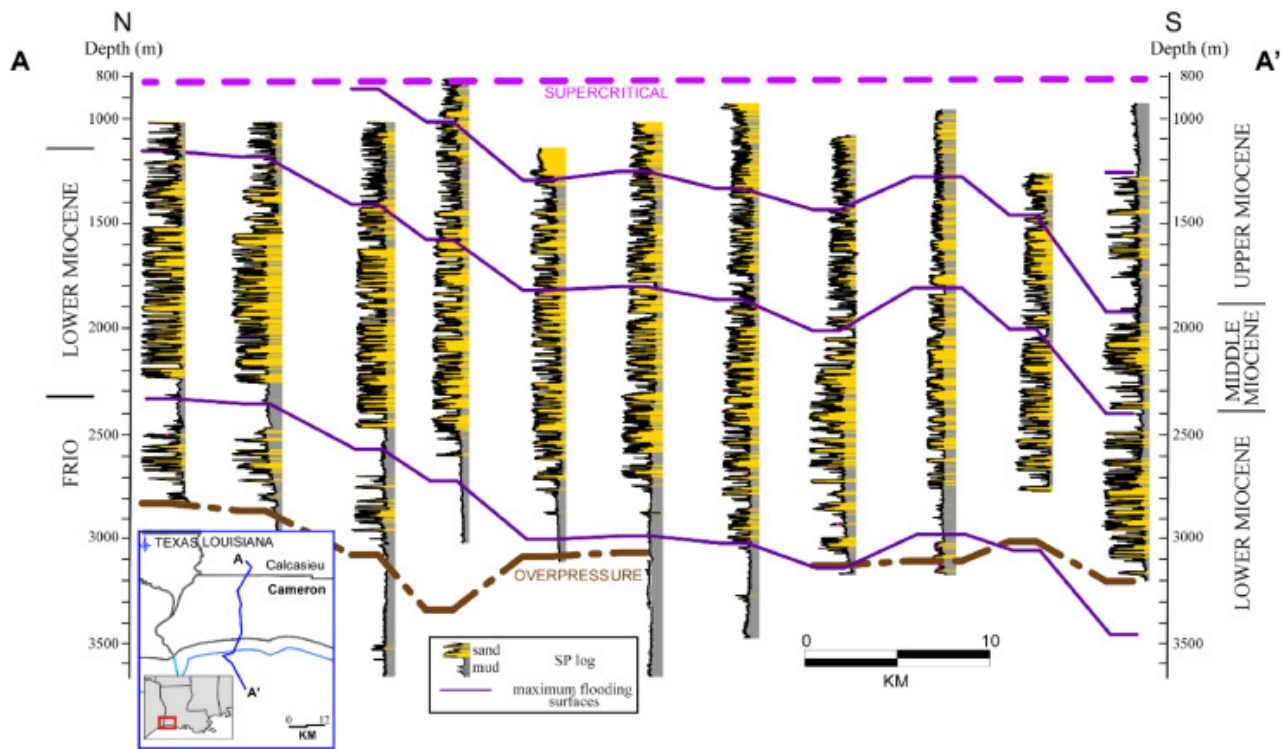
Fluid flow experiments were conducted at atmosphere temperature and pressure, using an analog fluid pair that has been calibrated to replicate the behavior of supercritical CO<sub>2</sub> and brine properties at typical subsurface storage reservoir CO<sub>2</sub> density and viscosity conditions (Krishnamurthy et al., 2019, 2022; Krishnamurthy, 2020; Niand Meckel, 2021). Specifically, we used heptane to represent supercritical CO<sub>2</sub> (the nonwetting phase) and a glycerol-water mixture to represent brine (the wetting phase). Note that the analog fluid pair chosen is immiscible so no dissolution trapping would be present. We initiated the experiment by injecting heptane through the center bottom inlet at a low flow rate (0.2 mL/min) so that the flow regime is strongly buoyancy- and capillary-dominated. Heptane was allowed to rise through the tank under buoyancy forces until it exited the top of the tank, concluding the drainage experiment. For the duration of the experiment, we used a high-resolution, monochrome camera to capture time-lapse images of the back-lit flow cell (Krishnamurthy et al., 2019, 2022; Krishnamurthy, 2020; Niand Meckel, 2021).

Fig. 2b is an image taken at the end of the experiment, showing the residual saturation and the flow path of the non-wetting fluid. There are several significant insights that emerge. First, we observe that flat, fine-grained layers retain buoyant fluid beneath them and can be regarded as barriers; they do not need to be anticlinal to trap CO<sub>2</sub>. Self-evidently, the amount of fluid retained would increase in proportion to the number and area of the barriers (or length of the barriers in the case of a two-dimensional experiment). Second, even very small capillary entry pressure contrasts can effectively divert flow of the buoyant, non-wetting phase. The contrast between coarse and medium sand is enough. The capillary entry pressure contrast between the matrix and the sand at the base of the fining up sequence in the barrier is 0.85 for the top layer and 0.74 for the middle layer, corresponding to a  $k_v/k_h$  ratio of 0.7 and 0.5 respectively. Last, gradation within the fine-grained layers has little impact on the amount of nonwetting phase fluid retained beneath—the buoyant phase gets diverted by the first capillary entry pressure contrast.

With respect to the performance of real-world composite confining systems, these results suggest that even changes in sand grain size (while having non-trivial porosity, permeability, and capillary entry threshold pressure) could offer effective barriers for impeding upward migration of the buoyancy-driven CO<sub>2</sub> plume. The experiment also suggests that barrier area and the number of barriers are important variables.

## 5. Characterizing subsurface barriers

Southern Louisiana offers a useful example to probe the geologic character of a potential composite confining system. Over a century of oil and gas production proves the quality of local reservoirs and creates a rich subsurface dataset. The “storage window” for CO<sub>2</sub> (Bump et al., 2021) is defined by pressure (depth below top of the water column) and the depth of the lowest USDW (Underground Source of Drinking Water, defined as <10,000 ppm Total Dissolved Solids; UIC Class VI 2010; USEPA 2013). At a minimum, injection must be deeper than the lowest USDW. Beyond that, maximizing storage efficiency suggests keeping injected CO<sub>2</sub> in a supercritical state, i.e., deeper than ~800 m below the top of the water column. At its base, the storage window is defined by the shallower of geologic overpressure or basement. In Southern Louisiana, the storage window extends from 800 to ~3000 m depth. Within that range, the local geology is dominated by sand-rich Miocene deltaic and shore zone deposits with large numbers of interbedded mudstones but no regionally extensive shale-rich seals (Fig. 3; Snedden and Galloway 2019; Bump et al. 2021).



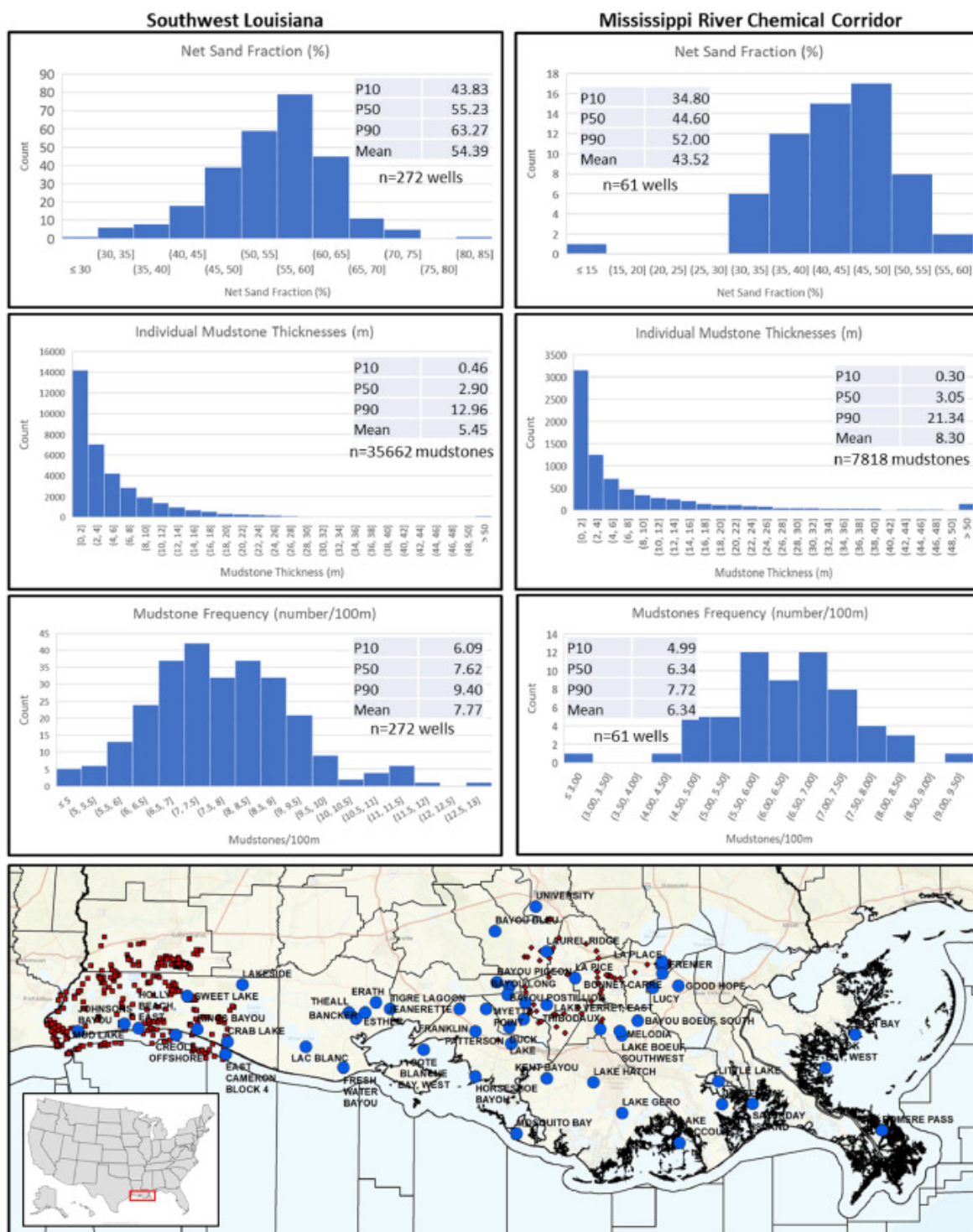
[Download : Download high-res image \(1MB\)](#)

[Download : Download full-size image](#)

Fig. 3. North-South-oriented cross-section showing the geology of southwestern Louisiana. The storage window for CO<sub>2</sub> is defined by the minimum depth for supercritical CO<sub>2</sub> (~800m; pink dashed line) and the top of overpressure (brown dashed line). Within the window, the geology is dominantly Miocene deltaic deposits, with frequent mudstones but no regionally-extensive seals. Stratigraphic correlations are shown for reference (purple lines).

We evaluated Spontaneous Potential (SP) logs from 323 wells in Southern Louisiana that record a total of over 40,000 individual mudstones within Miocene deltaic and shore zone facies (Fig. 4). We defined 2 facies –sand and mud, based on the SP log response. Log values were normalized to a range of -80 to +20 MV and a cutoff value of -30MV was used to differentiate sandy facies from muddy facies. As shown in Fig. 4, individual mud layers are thin. The median thickness is just over 3m and very few are more than 100m. What they lack in thickness however, they make up in numbers. On average, there are 6–8 mudstones per 100m of section across over 2km of stratigraphic section. While the histograms show wide variation (Fig. 4), the vast majority of observations are remarkably consistent: at the P10 level, there are 5–6 mudstones per 100m and at the P90 level, there are 8–9. In light of our sand tank experiments and the fact that some of these mudstones are proven hydrocarbon seals, we interpret all of them as barriers to the vertical migration of CO<sub>2</sub>.



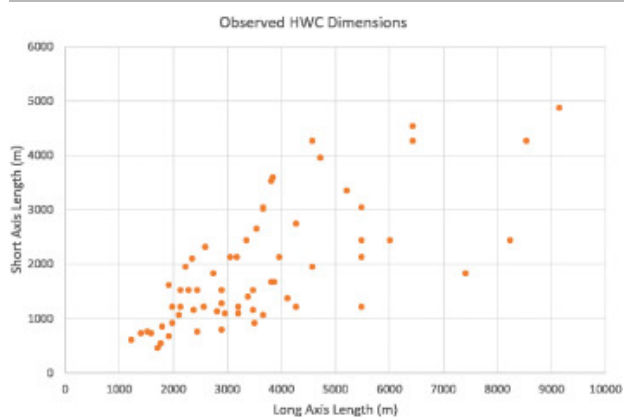


[Download : Download high-res image \(2MB\)](#)

[Download : Download full-size image](#)

Fig. 4. Characteristics of Southern Louisiana Miocene mudstones interpreted from SP logs. Map shows locations of wells (red dots) and fields (blue circles) used in this study. “Southwest Louisiana” refers to the 272 wells in the southwestern corner of the state (left-hand side of the map, square markers) and “Mississippi River Chemical Corridor” refers to the eastern cluster with 61 wells (center of the map, diamond markers).

Quantifying the lateral extent of individual mud layers is challenging. Correlating mud layers between wells is difficult at best and interpretations are generally non-unique. However, thanks to the presence of mobile salt, the area is heavily structured and nearly every structural high features a producing hydrocarbon field. While the specific sealing layers themselves are not mapped, the hydrocarbon-water contacts (HWC's) are and their footprints give minimum lateral extents for the overlying seals. Published reports from 63 fields in the Miocene deltaic and shore zone facies of Southern Louisiana show map-view field lengths (producing areas) ranging from ~1 km up to ~9 km along the long axis, with aspect ratios of ~2:1 (Fig. 5; McCampbell et al. 1964; Collier 1965, 1967; Harrison et al. 1970; McCormick 1983; Anderson et al. 1989; Christina and Corona 2010; Edmond et al. 2011). To be clear, the size of the field, and therefore the area of the HWC, is governed by the weakest link in a chain of factors that includes hydrocarbon charge volume, trap volume, capillary entry pressure of the seal and lateral extent of the seal. The lateral dimensions reported here are clearly minimums for the sealing mudstones—the aspect ratios of the hydrocarbon accumulations are all structurally controlled and it is likely that the extents of their seals are larger than the footprint of the HWC to an unknown extent that could be defined by a depositional pinch-out, an erosional scour or a fault truncation. Nevertheless, the HWC's are a useful constraint as they clearly show mudstone lengths an order of magnitude greater than those documented by outcrop studies (Zeito, 1965; Verriën et al., 1967).



[Download : Download high-res image \(123KB\)](#)

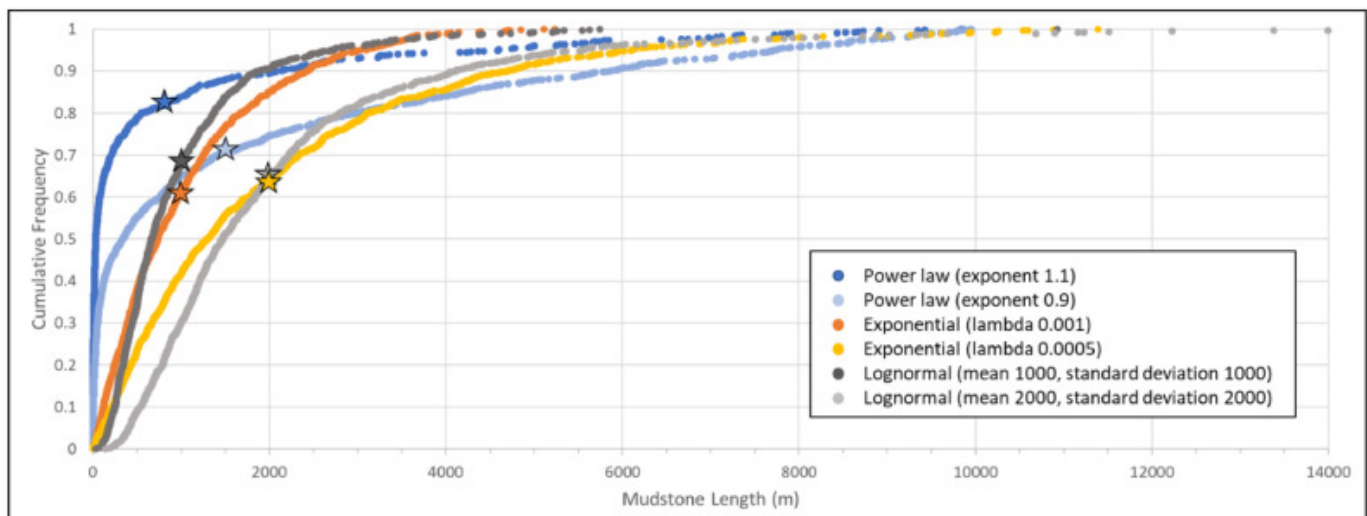
[Download : Download full-size image](#)

Fig. 5. Long and short axis dimensions of 67 HWC's from 63 producing fields in Southern Louisiana (see Fig. 4 for locations). Note that the aspect ratios are all structurally controlled and that field sizes may be limited by any of a number of factors. The dimensions shown here are thus interpreted minima for the overlying seals.

To constrain average barrier length for the calculation of  $k_v/k_h$  (Eq. (1)), we need to estimate a cumulative distribution function (CDF). We start with the observation that the published reports for each of the producing fields document 1–2 HWC's (and therefore the presence of field-scale mudstones) over 2.5 km of Miocene stratigraphic section. Based on the observed median (P50) value of 7 mudstones/100 m, we would expect 175 mudstones in that interval, meaning that proven field-scale seals occur ~0.5–1% of the time. However, we note that this is probably a significant underestimate of the actual occurrence. Among the 63 fields in this study, the median field produces from 11 separate reservoirs and 2 fields produce from over 50 reservoirs. If the unpublished producing intervals have seals of similar size, then the occurrence rate jumps

to ~6% (11 field-scale mudstones out of 175 total mudstones). In all likelihood, that too is an underestimate—there are probably also similar mudstones that invisible to our analysis, either because they are mis-aligned with the trap and thus incapable of sealing a field, or because the underlying sands were never charged. Their inclusion would further raise our estimate of the occurrence rate. Based on this, we conservatively estimate that field-scale (multi-kilometer length) mudstones occur at least 10% of the time (P90 occurrence).

The shape of the CDF is suggested by published works on ancient deltaic mudstone lengths as well as work on modern deltaic island areas—the analog areas for possible mudstone preservation (Zeito, 1965; Burton and Wood, 2011; Edmond et al., 2011). Both show log-normal distributions, with many more short mudstones than long ones. Fig. 6 explores possible CDFs for barrier lengths, using 1000 randomly generated lengths for a variety of functions. In the spirit of open-mindedness, we include not only log-normal curves, but also exponential and power law realizations. Each is guided by the idea that the curves should bracket a P90 length range of 2–5 km and that the longest lengths should be somewhat over 9 km. The resulting curves clearly span a range of shapes that may be more or less plausible. However, we note that in all cases, the average mudstone length is 0.8–2.0 km, driven by the long tails of the CDF's.



[Download : Download high-res image \(388KB\)](#)

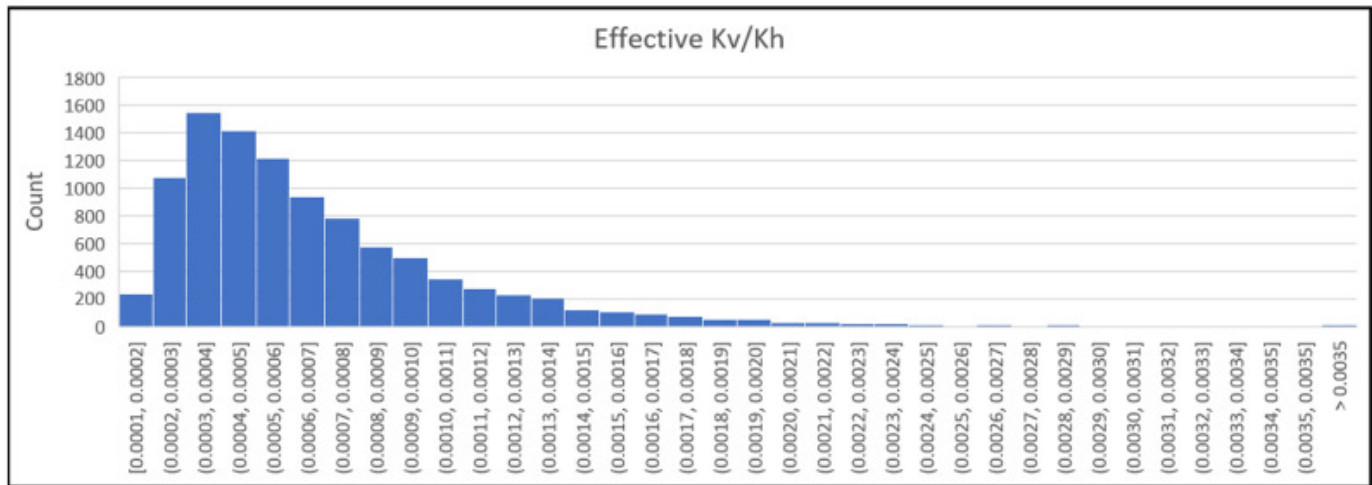
[Download : Download full-size image](#)

Fig. 6. Possible cumulative distribution functions for mudstone barrier lengths (long axis), given a minimum length of 1 m. Each curve shows 1000 randomly generated realizations, using a different function. Stars show the average length for each distribution.

Plugging these values into Eqs. (1) and (2) and using a Monte Carlo simulation gives an effective  $k_v/k_h$  range of 0.0001–0.0025 (Fig. 7). Implicit in this analysis is the assumption that there are enough barriers present that the mean lengths derived here are valid. Our numerical experiments suggest that 20–30 barriers are enough to assure convergence to within a few hundred meters of the mean. For the stratigraphy described above, with a median of ~7 documented barriers/100m, that would require ~400m of section for the average barrier length to reliably converge on the mean.

Confining Zone Parameters					
	N:G (fraction)	avg. shale length (m)	number of shales/100m	sand kv/kh	avg. shale aspect ratio (W:L)
Min	0.3	800	4	0.1	0.5
Most Likely	0.5	1400	8	0.3	0.7
Max	0.8	2000	12	0.6	0.9

Effective Kv/Kh	
p10	0.0002710
P50	0.0005511
P90	0.0012278
Mean	0.0006726



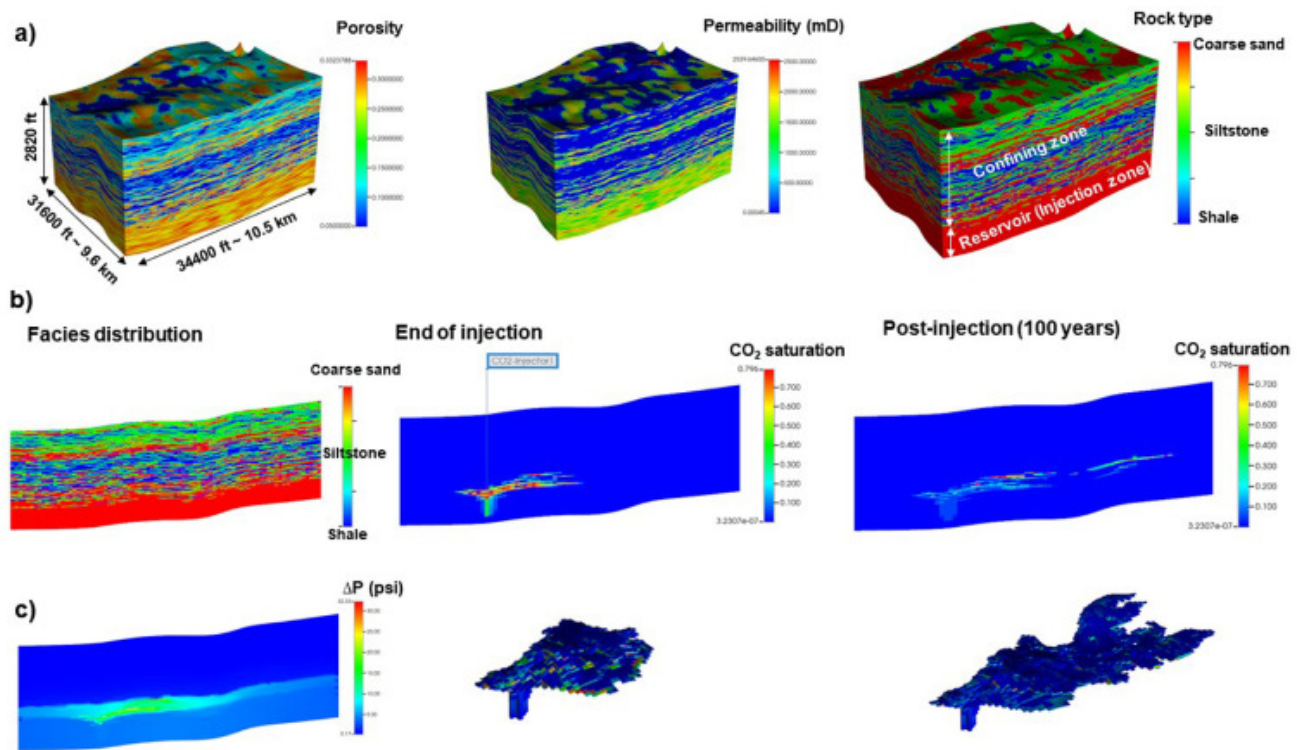
[Download : Download high-res image \(723KB\)](#)

[Download : Download full-size image](#)

Fig. 7. Monte Carlo simulation of effective  $k_v/k_h$  using Eqs.(1) and (2) and input parameters derived from observations of Southern Louisiana Miocene deltaic and shore zone facies. Sand  $k_v/k_h$  refers to the intrinsic permeability ratio of the sand flow units (0.1 is commonly used in reservoir engineering (e.g., [Elfenbein et al. 2005](#))).

## 6. Full-scale reservoir modeling

To test the ideas developed in the preceding sections, we employed a 3D geocellular model of the Louisiana coastal Miocene section. The model measures 9.6kmx10.5kmx0.9km and was originally built as a faithful representation of an actual storage prospect, located on the flank of an anticline with a 2° dip (Fig. 8a). The model is composed of a 570 ft-thick (174m) injection zone, overlain by a confining zone with a thickness of 2250ft (686m). The injection interval is composed of 98% coarse sand and the confining zone is populated with the same coarse sand, interbedded with discontinuous siltstones and mudstones. Synthetically generated facies curves (well pointsets) were used to model facies and lithotype distributions from 35 well locations within the model. For the confining interval, these well pointsets had a uniform mixture of sand (35%), shaly sand (32%), and shale (33%) litho-facies labels, distributed consistent with locally observed geologic stacking patterns. Using a plurigaussian simulator, multiple realizations were built from these pointsets to create realistic shale and sand distributions within the static model. Shale facies distributions were initially built with a primary axial length of 3000ft and a minor axial length of 750ft (229m) with a vertical thickness of 30ft (9m). The mudstones were assigned an average length of 5000ft (1524m) and the capillary entry pressure values for the coarse sandstone, siltstone, and shale are considered to be 0.2, 1.5, and 1488 psi, respectively ([Beckham et al., 2018](#)). CO<sub>2</sub> and brine relative permeability and drainage capillary pressure curves were generated using the Brooks-Corey model.



[Download : Download high-res image \(1MB\)](#)

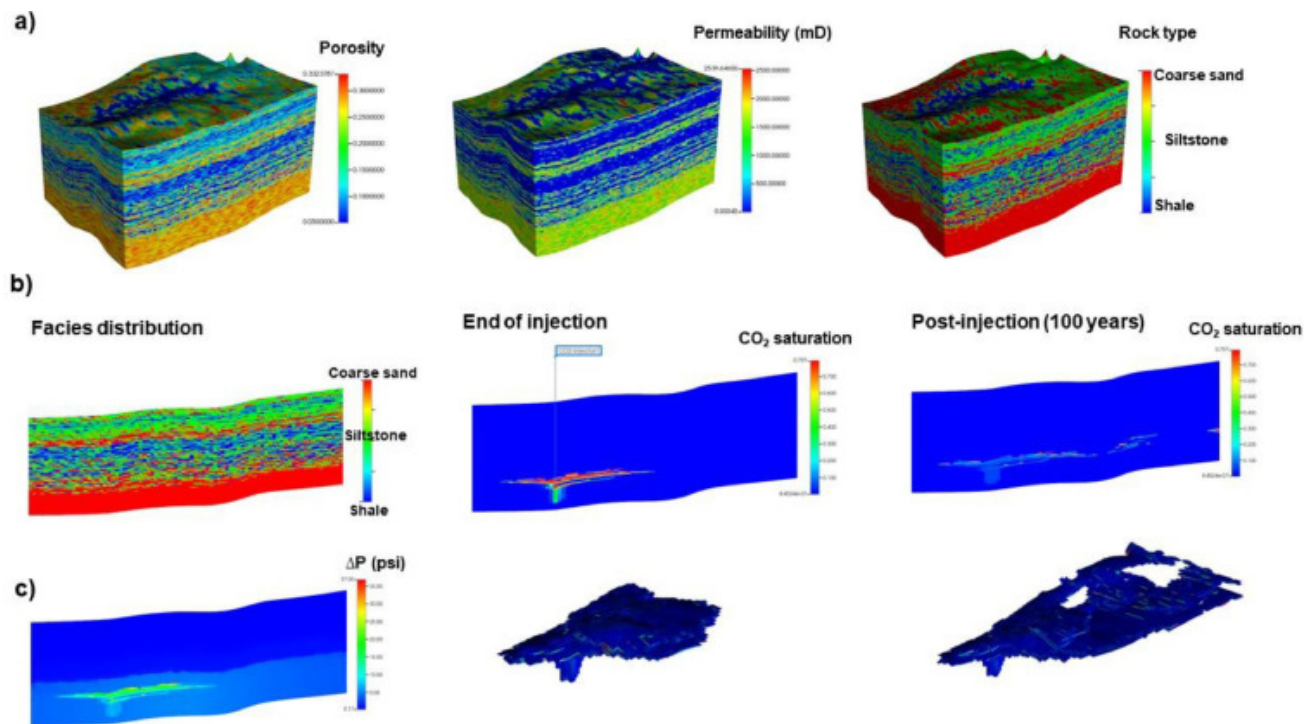
[Download : Download full-size image](#)

Fig. 8. Geocellular model and fluid flow simulation results using barriers of 5000ft (1524m) average length. (A) Porosity, permeability, and facies distributions in a model with the average capillary barriers length of 5000ft in the confining zone; (B) Cross-sections through the model showing facies distribution (left) and CO<sub>2</sub> saturation profile at the end of injection (middle) and 100 years post-injection (right); (C) pressure buildup at the end of the injection period ( $\Delta P$ ; left hand image) and 3D views of the CO<sub>2</sub> plume at the end of injection period (middle) and 100 years post-injection (right). Note that the pressure plume is primarily concentrated in the lower parts of the confining zone, indicating that the presence of barriers restricts the vertical communication of pressure.

Numerical injection simulations were conducted using GEM (<https://www.cmgl.ca/gem>) and Darcy flow, considering pure CO<sub>2</sub> and brine. The final model contains 1,485,440 grid blocks. All boundaries are taken to be closed and initial pore pressure is set to hydrostatic with the gradient of 10.5MPa/km (0.456psi/ft). CO<sub>2</sub> was injected downdip for 30 years in the reservoir with an injection rate of 59 mmscf/day (1.14Mt/yr). The simulations were continued for 100 years after the injection stopped. Fig.8 (b and c) shows the CO<sub>2</sub> plume at the end of injection and post-injection. Despite the lack of a continuous seal or even a continuous barrier, CO<sub>2</sub> makes very little vertical progress into the confining system. Rather, it tends to channelize underneath the capillary barriers, including both the silty and muddy facies. Similar to the sand tank experiments, CO<sub>2</sub> spreads laterally beneath the barriers, with significant residual trapping that attenuates and ultimately immobilizes the plume.

To explore the effect of barrier length on the CO<sub>2</sub> migration, we repopulated the confining zone with shorter barriers (average length of ~2000ft; 610m) and ran the simulation a second time (Fig.9). Even with shorter baffles, the confining zone is highly effective. As before, migration is dominantly lateral, following the

stratigraphic layering up-dip. Surprisingly, the vertical migration of the CO<sub>2</sub> plume in this case is even lower than the that for the case of 5000ft barriers. This counterintuitive result comes from the stochastic distribution of barriers in the two models, which happened to create a particularly sandy section at the base of the confining zone in the first model. Although the longer barriers are generally more effective at arresting vertical migration, that sandy zone (largely devoid of long barriers) acted more like the injection zone, offering little resistance to vertical flow and thus increasing the thickness of confining zone required.



[Download : Download high-res image \(869KB\)](#)

[Download : Download full-size image](#)

Fig. 9. Geocellular model and fluid flow simulation results using barriers of 2000ft (610m) average length. (A) Porosity, permeability, and facies distributions in a model with the average capillary barriers length of 2000ft in the confining zone; (B) Cross-sections through the model showing facies distribution (left) and CO<sub>2</sub> saturation profile at the end of injection (middle) and 100 years post-injection (right); (C) pressure buildup at the end of the injection period ( $\Delta P$ ; left hand image) and 3D views of the CO<sub>2</sub> plume at the end of injection period (middle) and 100 years post-injection (right). Note that the pressure plume is primarily concentrated in the lower parts of the confining zone, indicating that the presence of barriers restricts the vertical communication of pressure.

## 7. Discussion

Although composite confinement per se is a new concept, at least two GCS projects have demonstrated its promise and its risks, intentionally or not. The Illinois Basin Decatur project has injected over 3Mt of CO<sub>2</sub> into the Cambrian Mt Simon formation, sealed by the regionally extensive Eau Claire shale. The injection zone is a relatively high permeability zone in the lowest part of the Mt Simon, but between that and the seal is a heterogeneous zone of discontinuous, layered permeability contrasts, with heavily cemented, low-

permeability streaks interbedded with less-cemented, higher-permeability layers. History matched reservoir models, calibrated by repeat [seismic surveys](#), indicate that vertical migration of the injected CO<sub>2</sub> has been slowed or perhaps stopped by these intermediate layers. At present, the CO<sub>2</sub> plume remains entirely within the lower Mt Simon.

Sleipner provides a similar example. The injection zone (the Utsira sand) is an extremely high-quality reservoir with Darcy-scale permeability and a log character as homogeneous as any. However, repeat seismic surveys have shown that the injected CO<sub>2</sub> plume has evolved 9 distinct layers, the lowest 8 of which are interpreted to be ponding beneath meter-scale intraformational silts ([Cowton et al., 2016](#); [Williams and Chadwick, 2021](#)). If these silts were either more numerous or the holes in them were more randomly arranged, they might form an effective composite confining system. However, forensic [seismic analysis](#) indicates the presence of multiple vertical chimneys that breach all 8 barriers. The best-resolved of these is interpreted to be ~30m in diameter, with a vertical permeability of 100mD ([Chadwick et al., 2019](#)). The net result is an illustration of both the advantages and the risks of composite confining systems. On the plus side, the presence of the silt layers has probably limited the lateral spread of CO<sub>2</sub>, which is inconsequential for Sleipner but could reduce the monitoring footprint and lease requirements for a more constrained project. On the other hand, even with the silt layers, CO<sub>2</sub> reached the base of the seal (the Nordland shale) in only three years, illustrating the consequences of aligned holes and/or pervasive fractures in the barriers ([Cavanagh and Haszeldine, 2014](#); [Chadwick et al., 2019](#)). That is clearly a risk that needs to be addressed, both for composite confining systems and for conventional seals.

We believe that we have been conservative in our descriptions of both real and modelled composite confining systems as we have A) focused on the mud layers and B) been able to constrain only minimum mud lengths. Petroleum exploration shows that at least some of the Southern Louisiana barriers described here retain hydrocarbon columns of 10's to even 100's of meters, indicating high capillary entry pressures. However, as the sand tank experiments show, even very low capillary entry pressure contrasts are sufficient to divert the flow of CO<sub>2</sub> at low pressure. At distances from the well sufficient to dissipate [injection pressure](#), we expect that subtler variations in sand grain size will add greatly to the number of effective barriers and perhaps add to the length of those barriers identified here.

Even with the conservative statistics described here however, we struggle to create significant vertical migration in our 3D models. When we drive the models to failure, it occurs laterally—CO<sub>2</sub> exits the sides of the model rather than vertically through the confining system. To get CO<sub>2</sub> into the shallow section (where USDW might be present), we find that we need a means of shortcutting the tortuous flow path created by layered stratigraphy. This could take several forms—an open [wellbore](#), a permeable fault zone, fluid escape pipes or something similar. Even with such weaknesses, the amount of CO<sub>2</sub> leaked from the storage complex would depend on how much finds its way to the shortcut. The way that composite confinement tends to spread CO<sub>2</sub> could minimize that. Conceptually, [leakage](#) might also occur if there were persistent vertical alignment of homogeneous sand deposits that lacked the permeability contrasts to divert CO<sub>2</sub> laterally. Given the minimal contrasts needed to divert CO<sub>2</sub> however, it seems hard to envision a realistic scenario where this might happen. We worry more about steep dips and high-relief buoyant traps. Steep dips (e.g., on the flank of a salt diapir) could allow significant vertical migration without the need to cross stratigraphic barriers, effectively bypassing the confining system. High-relief buoyant traps could concentrate injected CO<sub>2</sub> and allow it to build the column height needed to breach barriers and thus the

shortcut the intended flow path. These are all clear, but familiar risks that can be addressed with good geologic characterization. Targeting flat-lying or gently-dipping systems, remote from permeable faults or fluid escape pipes, would minimize such risks.

The harder task may be allaying the worries of operators, investors, regulators and other stakeholders. Work on the Southwest Hub (Australia) project extensively explored the composite confining concept but did not test retention via injection (Sharma *et al.*, 2017; Sharma and Van Gent, 2018; Bourdet *et al.*, 2019). Well-documented examples from Sleipner and Decatur help to show the effectiveness of intraformational barriers under actual injection but no project has yet conclusively proven performance in confining zones (Cavanagh and Haszeldine, 2014; Sene *et al.*, 2014; Cowton *et al.*, 2016; Greenberg *et al.*, 2017; Freiburger *et al.*, 2022). We suggest a staged approach. First, characterize the confining system, similar to what we have done here, retaining the uncertainties and paying particular attention to potential fast paths across stratigraphic layering. Second, push the models to failure—find out what it takes to create an unacceptable outcome and either acquire the data to rule out that possibility or modify the injection strategy to reduce the risk. Finally, design the monitoring plan to target potential failure paths and pick up developing hazards early. It is important to note that we expect injected and displaced fluids to invade the lower parts of the confining zone. Because permeable zones are present within the composite confining system, monitoring pressure and saturation at multiple depths would be an effective way to monitor the progress of invasion and validate modeled performance, effectively reducing containment risk in a timely fashion.

Last, there is the question of retention capacity. Any confining system, be it a conventional shale seal or a composite system, has its limits. For conventional shale seals, this is usually expressed in terms of pressure differential or column height, which can be converted to volume, given knowledge of the trap geometry (e.g., Daniel and Kaldi 2008; Petersen *et al.* 2022). For composite confining systems, thickness of the system, and the average length of the barriers are clearly good starting points but conversion to retention volume will require modeling, including sensitivity analysis. The work presented here has focused on the effects of horizontal barriers, but ultimately, composite confinement relies on migration-assisted trapping—the sum of residual trapping, dissolution, local capillary trapping and local buoyant trapping within the flow units.

In contemplating the potential effectiveness of these processes, petroleum migration offers a useful analogy. Petroleum explorers have long accepted that some fraction of generated hydrocarbons is lost in migration from source rock to trap. Estimates of migration loss vary widely, from a few percent or less where high-permeability carrier beds offer an efficient path, up to 100% where charge is limited and migration occurs by vertical movement through layered, low-permeability units that attenuate significant volumes, so-called “waste zones” in the language of petroleum (Schowalter and Hess, 1982; Hirsch and Thompson, 1995; Lewan *et al.*, 1995; Sylta, 2002; Cornford, 2005). Migration through such zones may ultimately succeed only because of the very large volumes of petroleum generated, which can be as high as 10's or even 100's of millions of barrels per square kilometer of mature source rock (Lewan *et al.*, 1995; Aqrabi and Badics, 2015; Zetaware, 2022). Even so, migration through such systems is slow—the time lag between the onset of hydrocarbon generation in a source rock and the charging of shallower traps may be on the order of millions to even tens of millions of years (He and Murray, 2020). On a human timescale, migration at that speed is effectively permanent trapping.

With regard to predicting the effectiveness of migration-assisted trapping for CO<sub>2</sub>, storage efficiency numbers developed for static capacity estimation might be regarded as a baseline expectation, ~5%



(Gorecki *et al.*, 2009; Goodman *et al.*, 2011; Bachu, 2015). Beyond that, there are a number of factors that could modify predictions. Physical analog experiments and numerical models show that flow unit heterogeneity is a key variable. Features as subtle as cross-beds can radically alter the flow of CO<sub>2</sub>, changing sweep efficiency from ~1% of the pore space to ~40% or more (Krishnamurthy *et al.*, 2022). Similarly, roughness on the upper surface of the flow unit creates small buoyant traps that together can immobilize significant volumes of CO<sub>2</sub> (Gasda *et al.*, 2013). Even subtle variations in capillary entry pressure, such as might be found in poorly-sorted channel deposits, create local barriers that each trap a bit of CO<sub>2</sub> (Saadatpoor *et al.*, 2010). In short, flow unit heterogeneity is a clear asset for composite confining systems and it may increase retention capacity far above the static capacity baseline. Ultimately, modeling will be needed to assure retention capacity but historic CO<sub>2</sub> injection projects—e.g., Decatur, Quest, Frio and Ketzin—have shown that capillary trapping is highly effective (Hovorka *et al.*, 2006; Daley *et al.*, 2008; Martens *et al.*, 2013; Sene *et al.*, 2014).

## 8. Conclusion

Experience with subsurface petroleum reservoirs proves the capability of geologic traps and seals to retain buoyant fluids for geologic time. Historic GCS projects have demonstrated the security of similar systems for storage of CO<sub>2</sub>. However, sedimentary geology does not always fit the preconceived ideal of petroleum-type reservoirs and seals. This work shows that it does not need to do so. Indeed, the goal of permanent sequestration may be better served by composite confinement than by classic petroleum seals that retain fluids in a concentrated, mobile state that could leak if given a path. The strength of composite confinement is that it takes advantage of common sedimentary layering to disperse and immobilize injected CO<sub>2</sub>, assuring permanent containment. Paradoxically, a sequence of discontinuous beds with modest capillary entry pressure contrast may offer lower leakage risk than classically perfect seals.

Offering a new paradigm for containment, composite confining systems can open new stratigraphy and new geography for GCS, reducing transport distances and project costs. The Mississippi River Chemical Corridor and the onshore region south of Perth, Australia are two such areas—rich in injectable reservoirs and point-source CO<sub>2</sub> emissions, but lacking classic regional seals. Composite confining systems enable local GCS. Indeed, projects already in development in these areas will rely on it.

Perhaps the most difficult aspect of composite confinement is convincing operators, investigators and/or regulators that it will. We suggest addressing this by pushing models to failure—find out what it takes to make the confining system fail. Much like crash testing allows the auto industry to explore failure and design safer vehicles, fluid flow modeling can explore the limits of confining systems and allow operators to design characterization, injection and monitoring programs to assure against possible failures. For those accustomed to thinking in terms of classic hydrocarbon seals, adoption of composite confining systems requires setting aside historic concepts of what “good” looks like. The possibility of a wider opportunity set and greater long-term security make that a prize worth chasing.

## CRedit authorship contribution statement

**Alexander P. Bump:** Conceptualization, Methodology, Investigation, Formal analysis, Supervision, Funding acquisition, Project administration, Writing – original draft, Writing – review & editing. **Sahar Bakhshian:** Methodology, Investigation, Formal analysis, Visualization, Writing – original draft, Writing – review &

editing. **Hailun Ni**: Methodology, Investigation, Formal analysis, Visualization, Writing – original draft, Writing – review & editing. **Susan D. Hovorka**: Supervision, Writing – review & editing. **Marianna I. Olariu**: Investigation, Visualization. **Dallas Dunlap**: Methodology. **Seyyed A. Hosseini**: Supervision. **Timothy A. Meckel**: Supervision.

## Declaration of Competing Interest

The authors declare that they have no known competing financial interests or personal relationships that could have appeared to influence the work reported in this paper.

## Acknowledgments

This work was funded by industrial sponsors of the Gulf Coast Carbon Center. The ideas presented have benefitted significantly from discussion with Charles Jenkins, Michael Sweet and John Snedden. Amanda Merida Rodriguez led the heroic effort to digitize the hundreds of well logs used here. Two anonymous reviewers significantly improved the quality of the manuscript. We thank them all.

[Recommended articles](#)

## Data availability

Data will be made available on request.

## References

[Agartan et al., 2017](#) E. Agartan, A. Cihan, T.H. Illangasekare, Q. Zhou, J.T. Birkholzer

Mixing and trapping of dissolved CO<sub>2</sub> in deep geologic formations with shale layers

Adv. Water Resour., 105 (2017), pp. 67-81, [10.1016/j.advwatres.2017.04.014](https://doi.org/10.1016/j.advwatres.2017.04.014) ↗

v

 [View PDF](#) [View article](#) [View in Scopus](#) ↗ [Google Scholar](#) ↗

[Agartan et al., 2015](#) E. Agartan, L. Trevisan, A. Cihan, J. Birkholzer, Q. Zhou, T.H. Illangasekare

Experimental study on effects of geologic heterogeneity in enhancing dissolution trapping of supercritical CO<sub>2</sub>

Water Resour. Res., 51 (2015), pp. 1635-1648, [10.1002/2014WR015778](https://doi.org/10.1002/2014WR015778) ↗

v

[View in Scopus](#) ↗ [Google Scholar](#) ↗

[Anderson et al., 1989](#) Anderson, A., Anderson, R., Carter, R., Dobie, C.W., and Fambrough, J.W. (eds.), 1989, Typical Oil & Gas Fields of Southwestern Louisiana, III: Lafayette, LA, Lafayette Geological Society.

[Google Scholar](#) ↗

[Aqrabi and Badics, 2015](#) A.A.M. Aqrabi, B. Badics

## Geochemical characterisation, volumetric assessment and shale-oil/gas potential of the Middle Jurassic–Lower Cretaceous source rocks of NE Arabian Plate

GeoArabia, 20 (2015), pp. 99-140, [10.2113/geoarabia200399](https://doi.org/10.2113/geoarabia200399) ↗

v

[View in Scopus ↗](#) [Google Scholar ↗](#)

[Bachu, 2015](#) S. Bachu

### Review of CO<sub>2</sub> storage efficiency in deep saline aquifers

Int. J. Greenh. Gas Control, 40 (2015), pp. 188-202, [10.1016/j.ijggc.2015.01.007](https://doi.org/10.1016/j.ijggc.2015.01.007) ↗

v

 [View PDF](#) [View article](#) [View in Scopus ↗](#) [Google Scholar ↗](#)

[Beckham et al., 2018](#) E.C. Beckham, T.A. Meckel, P.P. Flaig

### Investigating Deltaic Architecture and Reservoir Connectivity for CO<sub>2</sub> Storage and Migration: Integrated Perspectives from Physical Models of Flume Tank experiments, Outcrop analogs, and Subsurface Mapping

IEAGHG, Melbourne, Australia (2018), p. 14

[Google Scholar ↗](#)

[Begg et al., 1985](#) S.H. Begg, D.M. Chang, H.H. Haldorsen

### A Simple Statistical Method for Calculating the Effective Vertical Permeability of a Reservoir Containing Discontinuous Shales

SPE, Las Vegas (1985), p. 15

[Google Scholar ↗](#)

[Bourdet et al., 2019](#) Bourdet, J. et al., 2019, Assessment of multi-barrier systems for CO<sub>2</sub> containment in the Yalgorup Member of the Lesueur Sandstone, South West Hub: CSIRO CSIRO Report EP19286, 293 p.

[Google Scholar ↗](#)

[Bump et al., 2021](#) A.P. Bump, S.D. Hovorka, T.A. Meckel

### Common risk segment mapping: streamlining exploration for carbon storage sites, with application to coastal Texas and Louisiana

Int. J. Greenh. Gas Control, 111 (2021), Article 103457, [10.1016/j.ijggc.2021.103457](https://doi.org/10.1016/j.ijggc.2021.103457) ↗

v

 [View PDF](#) [View article](#) [View in Scopus ↗](#) [Google Scholar ↗](#)

[Burton and Wood, 2011](#) D. Burton, L.J. Wood

### Quantitative shale characterization of the tidally influenced sego sandstone

Am. Assoc. Pet. Geol. Bull., 95 (2011), pp. 1207-1226, [10.1306/12081010119](https://doi.org/10.1306/12081010119) ↗

v

[View in Scopus ↗](#) [Google Scholar ↗](#)

[Cavanagh and Haszeldine, 2014](#) A.J. Cavanagh, R.S. Haszeldine

## The Sleipner storage site: capillary flow modeling of a layered CO<sub>2</sub> plume requires fractured shale barriers within the Utsira Formation

Int. J. Greenh. Gas Control, 21 (2014), pp. 101-112, [10.1016/j.ijggc.2013.11.017](https://doi.org/10.1016/j.ijggc.2013.11.017) ↗

v

 [View PDF](#) [View article](#) [View in Scopus ↗](#) [Google Scholar ↗](#)

[Chadwick et al., 2019](#) R.A. Chadwick, G.A. Williams, I. Falcon-Suarez

## Forensic mapping of seismic velocity heterogeneity in a CO<sub>2</sub> layer at the Sleipner CO<sub>2</sub> storage operation, North Sea, using time-lapse seismics

Int. J. Greenh. Gas Control, 90 (2019), Article 102793, [10.1016/j.ijggc.2019.102793](https://doi.org/10.1016/j.ijggc.2019.102793) ↗

v

 [View PDF](#) [View article](#) [View in Scopus ↗](#) [Google Scholar ↗](#)

[Christina and Corona, 2010](#) C. Christina, C. Corona

## Oil & Gas Fields of South Louisiana

New Orleans Geological Society, New Orleans, Louisiana (2010), p. 318

2010

[Google Scholar ↗](#)

[Collier, 1965](#) H.G. Collier

Oil and Gas Fields of Southeast Louisiana, 1, New Orleans Geological Society, New Orleans, Louisiana (1965), p. 159

[Google Scholar ↗](#)

[Collier, 1967](#) H.G. Collier

Oil and Gas Fields of Southeast Louisiana, 2, New Orleans Geological Society, New Orleans, Louisiana (1967), p. 140

[Google Scholar ↗](#)

[Cornford, 2005](#) C. Cornford

## Petroleum geology | the petroleum system

Encyclopedia of Geology, Elsevier (2005), pp. 268-294, [10.1016/B0-12-369396-9/00247-1](https://doi.org/10.1016/B0-12-369396-9/00247-1) ↗

 [View PDF](#) [View article](#) [Google Scholar ↗](#)

[Cowton et al., 2016](#) L.R. Cowton, J.A. Neufeld, N.J. White, M.J. Bickle, J.C. White, R.A. Chadwick

## An inverse method for estimating thickness and volume with time of a thin CO<sub>2</sub>-filled layer at the Sleipner Field, North Sea

J. Geophys. Res. Solid Earth, 121 (2016), pp. 5068-5085, [10.1002/2016JB012895](https://doi.org/10.1002/2016JB012895) ↗

v

[View in Scopus ↗](#) [Google Scholar ↗](#)

[Daley et al., 2008](#) T.M. Daley, L.R. Myer, J.E. Peterson, E.L. Majer, G.M. Hoversten

## Time-lapse crosswell seismic and VSP monitoring of injected CO<sub>2</sub> in a brine aquifer

Environ. Geol. (2008), p. 9

[View in Scopus ↗](#) [Google Scholar ↗](#)

**Daniel and Kaldi, 2008** Daniel, R.F., and Kaldi, J.G., 2008, Evaluating seal capacity of caprocks and intraformational barriers for the geosequestration of CO<sub>2</sub>, p. 11.

[Google Scholar ↗](#)

**Dermansky, 2023** Dermansky, J., 2023, The battle to stop air products' carbon capture project at lake Maurepas grows: DeSmog, <https://www.desmog.com/2023/02/17/air-products-lake-maurepas-louisiana-ccs-blue-hydrogen/> ↗ (accessed April 2023).

[Google Scholar ↗](#)

**Directive 2009/31/EC 2009** Directive 2009/31/EC, 2009, Directive 2009/31/EC of the European Parliament and of the Council of 23 April 2009 on the geological storage of carbon dioxide and amending Council Directive 85/337/EEC, European Parliament and Council Directives 2000/60/EC, 2001/80/EC, 2004/35/EC, 2006/12/EC, 2008/1/EC and Regulation (EC) No 1013/2006: p. L140:114-35, doi:10.1007/978-1-137-54507-7\_21.

[Google Scholar ↗](#)

**Downey, 1994** M. Downey

### Hydrocarbon seal rocks

The Petroleum System—From Source to Trap, 60, American Association of Petroleum Geologists, AAPG Memoir, Tulsa, Oklahoma (1994), pp. 159-164, [10.1306/M60585C8](https://doi.org/10.1306/M60585C8) ↗

v

[View in Scopus ↗](#) [Google Scholar ↗](#)

**Edmonds et al., 2011** D.A. Edmonds, C. Paola, D.C.J.D. Hoyal, B.A. Sheets

### Quantitative metrics that describe river deltas and their channel networks

J. Geophys. Res., 116 (2011), p. F04022, [10.1029/2010JF001955](https://doi.org/10.1029/2010JF001955) ↗

v

[View in Scopus ↗](#) [Google Scholar ↗](#)

**Elfenbein et al., 2005** C. Elfenbein, Ø. Husby, P. Ringrose

### Geologically based estimation of $k_v/k_h$ ratios: an example from the Garn Formation, Tyrihans Field, Mid-Norway: Geological Society, London

Proceedings of the Petroleum Geology Conference Series, 6 (2005), pp. 537-543, [10.1144/0060537](https://doi.org/10.1144/0060537) ↗

v

[View in Scopus ↗](#) [Google Scholar ↗](#)

**Freiburg et al., 2022** J.T. Freiburg, M. Peltz, D.C. Willette, G.H. Grathoff

### High-resolution pore space imaging, mineralogical characterization, and sealing capacity estimates of confining units at a geologic carbon storage demonstration: the illinois basin–decatur project

USA J. Geol., 130 (2022), pp. 335-355, [10.1086/722563](https://doi.org/10.1086/722563) ↗

v

[View in Scopus ↗](#) [Google Scholar ↗](#)

[Gasda et al., 2013](#) S.E. Gasda, H.M. Nilsen, H.K. Dahle

### Impact of structural heterogeneity on upscaled models for large-scale CO<sub>2</sub> migration and trapping in saline aquifers

Adv. Water Resour., 62 (2013), pp. 520-532, [10.1016/j.advwatres.2013.05.003](#) ↗

v

 [View PDF](#) [View article](#) [View in Scopus](#) ↗ [Google Scholar](#) ↗

[Goodman et al., 2011](#) A. Goodman, *et al.*

### US DOE methodology for the development of geologic storage potential for carbon dioxide at the national and regional scale

Int. J. Greenh. Gas Control (5) (2011), pp. 952-965, [10.1016/j.ijggc.2011.03.010](#) ↗

v

 [View PDF](#) [View article](#) [View in Scopus](#) ↗ [Google Scholar](#) ↗

[Gorecki et al., 2009](#) C.D. Gorecki, J.A. Sorensen, J.M. Bremer, D. Knudsen, S.A. Smith, E.N. Steadman, J.A. Harju

### Development of storage coefficients for determining the effective CO<sub>2</sub> storage resource in deep saline formations

Proceedings of the SPE International Conference on CO<sub>2</sub> Capture, Storage, and Utilization, San Diego, California, USA, Society of Petroleum Engineers (2009), [10.2118/126444-MS](#) ↗

[Google Scholar](#) ↗

[Green and Ennis-King, 2010](#) C.P. Green, J. Ennis-King

### Effect of vertical heterogeneity on long-term migration of CO<sub>2</sub> in saline formations

Transp. Porous Media, 82 (2010), pp. 31-47, [10.1007/s11242-009-9498-7](#) ↗

v

[View in Scopus](#) ↗ [Google Scholar](#) ↗

[Green and Ennis-King, 2015](#) C.P. Green, J. Ennis-King

### Estimating breakthrough time during buoyant migration of CO<sub>2</sub> in a reservoir containing impermeable barriers

Transp. Porous Media, 107 (2015), pp. 281-298, [10.1007/s11242-014-0441-1](#) ↗

v

[View in Scopus](#) ↗ [Google Scholar](#) ↗

[Green and Ennis-King, 2013](#) C.P. Green, J. Ennis-King

### Residual trapping beneath impermeable barriers during buoyant migration of CO<sub>2</sub>

Transp. Porous Media, 98 (2013), pp. 505-524, [10.1007/s11242-013-0156-8](#) ↗

v

[View in Scopus](#) ↗ [Google Scholar](#) ↗

[Greenberg et al., 2017](#) S.E. Greenberg, R. Bauer, R. Will, R. Locke II, M. Carney, H. Leetaru, J. Medler

### Geologic carbon storage at a one million tonne demonstration project: lessons learned from the Illinois basin – Decatur project

Energy Procedia, 114 (2017), pp. 5529-5539, [10.1016/j.egypro.2017.03.1913](#) ↗

V

[View PDF](#) [View article](#) [View in Scopus](#) [Google Scholar](#)[Grunau, 1987](#) H.R. Grunau

### A worldwide look at the Caprock problem

J. Pet. Geol. (10) (1987), pp. 245-266

V

[CrossRef](#) [View in Scopus](#) [Google Scholar](#)[Harrison and Jones, 1970](#) F.W. Harrison, R.K. Jones, L.K. Searles

Typical Oil &amp; Gas Fields of Southwestern Louisiana, II, Lafayette Geological Society, Lafayette, LA (1970)

[Google Scholar](#)[Hart and Schlossberg, 2021](#) P. Hart, M. Schlossberg

### Top 5 reasons carbon capture and storage (CCS) is bogus

Food Water Watch (2021)

<https://www.foodandwaterwatch.org/2021/07/20/top-5-reasons-carbon-capture-and-storage-ccs-is-bogus/> accessed April 2023[Google Scholar](#)[Haszeldine and Scott, 2014](#) CHAPTER 2

R.S. Haszeldine, V. Scott, R.M. Harrison, R.E. Hester

### Storing carbon for geologically long timescales to engineer climate

Issues in Environmental Science and Technology, Royal Society of Chemistry, Cambridge (2014), pp. 22-51,

[10.1039/9781782621225-00022](https://doi.org/10.1039/9781782621225-00022)[View in Scopus](#) [Google Scholar](#)[He and Murray, 2020](#) Z. He, A. Murray

### Migration Loss, Lag and Fractionation

Implications for Fluid Properties and Charge Risk, Houston (2020), p. 22

[CrossRef](#) [View in Scopus](#) [Google Scholar](#)[Hirsch and Thompson, 1995](#) L.M. Hirsch, A.H. Thompson

### Minimum saturations and buoyancy in secondary migration

Am. Assoc. Pet. Geol. Bull., 79 (1995), pp. 696-710

V

[View in Scopus](#) [Google Scholar](#)[Holloway, 1996](#) S. Holloway

### The underground disposal of carbon dioxide

Final Report of the Joule II Project No. CT92-0031, Keyworth, British Geological Survey (1996), p. 355

[Google Scholar](#)[Hovorka et al., 2006](#) S.D. Hovorka, *et al.*

### Measuring permanence of CO<sub>2</sub> storage in saline formations: the Frio experiment

Environ. Geosci., 13 (2006), pp. 105-121, [10.1306/eg.11210505011](https://doi.org/10.1306/eg.11210505011) ↗

v

[View in Scopus](#) ↗ [Google Scholar](#) ↗

**IEAGHG 2011** IEAGHG, 2011, Caprock systems for CO<sub>2</sub> geological storage: IEAGHG 2011/01, 149 p., [https://ieaghg.org/publications/technical-reports/reports-list/9-technical-reports/1028-2011-01-caprock-systems-for-CO<sub>2</sub>-geological-storage](https://ieaghg.org/publications/technical-reports/reports-list/9-technical-reports/1028-2011-01-caprock-systems-for-CO2-geological-storage) ↗ (accessed April 2023).

[Google Scholar](#) ↗

**IEAGHG 2019** IEAGHG, 2019, The shell quest carbon capture and storage project: IEAGHG 2019/04, 186 p.

[Google Scholar](#) ↗

**ISO/TC 265 2017** ISO/TC 265, 2017, Carbon dioxide capture, transportation and geological storage – geological storage: International Standards Organization, 68 p.

[Google Scholar](#) ↗

**Kampman et al., 2016** N. Kampman, *et al.*

Observational evidence confirms modelling of the long-term integrity of CO<sub>2</sub>-reservoir caprocks

Nat. Commun., 7 (2016), p. 12268, [10.1038/ncomms12268](https://doi.org/10.1038/ncomms12268) ↗

v

[View in Scopus](#) ↗ [Google Scholar](#) ↗

**Krishnamurthy, 2020** P.G. Krishnamurthy

Geologic Heterogeneity Controls On CO<sub>2</sub> Migration and Trapping

The University of Texas at Austin (2020)

[Google Scholar](#) ↗

**Krishnamurthy et al., 2022** P.G. Krishnamurthy, D. DiCarlo, T. Meckel

Geologic heterogeneity controls on trapping and migration of CO<sub>2</sub>

Geophys. Res. Lett., 49 (2022), [10.1029/2022GL099104](https://doi.org/10.1029/2022GL099104) ↗

v

[Google Scholar](#) ↗

**Krishnamurthy et al., 2019** P.G. Krishnamurthy, T.A. Meckel, D. DiCarlo

Mimicking geologic depositional fabrics for multiphase flow experiments

Water Resour. Res., 55 (2019), pp. 9623-9638, [10.1029/2019WR025664](https://doi.org/10.1029/2019WR025664) ↗

v

[View in Scopus](#) ↗ [Google Scholar](#) ↗

**Leverett, 1941** M.C. Leverett

Capillary behavior in porous solids

Trans. AIME, 142 (1941), pp. 152-169, [10.2118/941152-G](https://doi.org/10.2118/941152-G) ↗

v

[Google Scholar](#) ↗



[Lewan et al., 1995](#) Lewan, M.D., Comer, J.B., Hamilton-Smith, T., Hasenmueller, N.R., Guthrie, J.M., Hatch, J.R., Gautier, D.L., and Frankie, W.T., 1995, Feasibility study of material-balance assessment of petroleum from the New Albany Shale in the Illinois Basin: USGS U.S. Geological Survey Bulletin 2137, 31 p.

[Google Scholar ↗](#)

[Lindeberg, 1997](#) E. Lindeberg

### Escape of CO<sub>2</sub> from aquifers

Energy Convers. Manag., 38 (1997), pp. S235-S240, [10.1016/S0196-8904\(96\)00275-0 ↗](#)

v

 [View PDF](#) [View article](#) [View in Scopus ↗](#) [Google Scholar ↗](#)

[Lu et al., 2009](#) J. Lu, M. Wilkinson, R.S. Haszeldine, A.E. Fallick

### Long-term performance of a mudrock seal in natural CO<sub>2</sub> storage

Geology, 37 (2009), pp. 35-38, [10.1130/G25412A.1 ↗](#)

v

[View in Scopus ↗](#) [Google Scholar ↗](#)

[Martens et al., 2013](#) S. Martens, *et al.*

### CO<sub>2</sub> storage at the Ketzin Pilot Site, Germany: fourth year of injection, monitoring, modelling and verification

Energy Procedia, 37 (2013), pp. 6434-6443, [10.1016/j.egypro.2013.06.573 ↗](#)

v

 [View PDF](#) [View article](#) [View in Scopus ↗](#) [Google Scholar ↗](#)

[McCampbell et al., 1964](#) J.C. McCampbell, J.W. Sheller, G.R. Maccaulay, J.W. Shirley

Typical Oil & Gas Fields of Southwestern Louisiana, I, Lafayette Geological Society, Lafayette, LA (1964), p. 1964 with Supplement, 1967

[https://books.google.com/books ↗](https://books.google.com/books)

?id=0ak\\_AAAAIAAJ

[Google Scholar ↗](#)

[McCormick, 1983](#) L.L. McCormick

### Oil and Gas Fields of Southeast Louisiana, Volume 3

New Orleans Geological Society, New Orleans, Louisiana (1983)

[Google Scholar ↗](#)

[Miocic et al., 2016](#) J.M. Miocic, S.M.V. Gilfillan, J.J. Roberts, K. Edlmann, C.I. McDermott, R.S. Haszeldine

### Controls on CO<sub>2</sub> storage security in natural reservoirs and implications for CO<sub>2</sub> storage site selection

Int. J. Greenh. Gas Control, 51 (2016), pp. 118-125, [10.1016/j.ijggc.2016.05.019 ↗](#)

v

 [View PDF](#) [View article](#) [View in Scopus ↗](#) [Google Scholar ↗](#)

Mullin, 2023 Mullin, R., 2023, The battle for Lake Maurepas: Chemical & Engineering News, <https://cen.acs.org/environment/battle-Lake-Maurepas/101/i11> ↗ (accessed April 2023).

[Google Scholar](#) ↗

Ni and Meckel, 2021 H. Ni, T.A. Meckel

Characterizing the effect of capillary heterogeneity on multiphase flow pulsation in an intermediate-scale beadpack experiment using time series clustering and frequency analysis

Water Resour. Res., 57 (2021), pp. 1-17, [10.1029/2021WR030876](https://doi.org/10.1029/2021WR030876) ↗

v

[View in Scopus](#) ↗ [Google Scholar](#) ↗

Nordbotten et al., 2009 J.M. Nordbotten, D. Kavetski, M.A. Celia, S. Bachu

Model for CO<sub>2</sub> leakage including multiple geological layers and multiple leaky wells

Environ. Sci. Technol., 43 (2009), pp. 743-749, [10.1021/es801135v](https://doi.org/10.1021/es801135v) ↗

v

[Google Scholar](#) ↗

Oldenburg, 2008 C.M. Oldenburg

Screening and ranking framework for geologic CO<sub>2</sub> storage site selection on the basis of health, safety, and environmental risk

Environ. Geol., 54 (2008), pp. 1687-1694, [10.1007/s00254-007-0947-8](https://doi.org/10.1007/s00254-007-0947-8) ↗

v

[View in Scopus](#) ↗ [Google Scholar](#) ↗

Oldenburg and Unger, 2003 C.M. Oldenburg, A.J.A. Unger

On leakage and seepage from geologic carbon sequestration sites: unsaturated zone attenuation

Vadose Zone J., 2 (2003), p. 10

v

[Google Scholar](#) ↗

Paluszny et al., 2020 A. Paluszny, C.C. Graham, K.A. Daniels, V. Tsaparli, D. Xenias, S. Salimzadeh, L. Whitmarsh, J.F. Harrington, R.W. Zimmerman

Caprock integrity and public perception studies of carbon storage in depleted hydrocarbon reservoirs

Int. J. Greenh. Gas Control, 98 (2020), Article 103057, [10.1016/j.ijggc.2020.103057](https://doi.org/10.1016/j.ijggc.2020.103057) ↗

v

 [View PDF](#) [View article](#) [View in Scopus](#) ↗ [Google Scholar](#) ↗

Petersen et al., 2022 H.I. Petersen, N. Springer, R. Weibel, N.H. Schovsbo

Sealing capability of the Eocene–Miocene Horda and Lark formations of the Nini West depleted oil field – implications for safe CO<sub>2</sub> storage in the North Sea

Int. J. Greenh. Gas Control, 118 (2022), Article 103675, [10.1016/j.ijggc.2022.103675](https://doi.org/10.1016/j.ijggc.2022.103675) ↗

v

[View PDF](#) [View article](#) [View in Scopus](#) [Google Scholar](#)

**Reason, 2000** Reason, J., 2000, Human error: models and management: v. 320, p. 3.

[Google Scholar](#)

**Roberts, 2020** Roberts, S., 2020, The swiss cheese model of pandemic defense: The New York Times, <https://www.nytimes.com/2020/12/05/health/coronavirus-swiss-cheese-infection-mackay.html> (accessed June 2022).

[Google Scholar](#)

**Saadatpoor et al., 2010** E. Saadatpoor, S.L. Bryant, K. Sepehrnoori

New trapping mechanism in carbon sequestration

Transp. Porous Media, 82 (2010), pp. 3-17, [10.1007/s11242-009-9446-6](https://doi.org/10.1007/s11242-009-9446-6)

v

[View in Scopus](#) [Google Scholar](#)

**Schincariol and Schwartz, 1990** R.A. Schincariol, F.W. Schwartz

An experimental investigation of variable density flow and mixing in homogeneous and heterogeneous media

Water Resour. Res., 26 (1990), pp. 2317-2329, [10.1029/WR026i010p02317](https://doi.org/10.1029/WR026i010p02317)

v

[View in Scopus](#) [Google Scholar](#)

**Schowalter and Hess, 1982** T.T. Schowalter, P.D. Hess

Interpretation of subsurface hydrocarbon shows

Am. Assoc. Pet. Geol. Bull., 66 (1982), pp. 1302-1327

v

[View in Scopus](#) [Google Scholar](#)

**Senel et al., 2014** O. Senel, R. Will, R.J. Butsch

Integrated reservoir modeling at the Illinois Basin - Decatur Project: integrated reservoir modeling: greenhouse Gases

Sci. Technol., 4 (2014), pp. 662-684, [10.1002/ghg.1451](https://doi.org/10.1002/ghg.1451)

v

[View in Scopus](#) [Google Scholar](#)

**Shappell and Wiegmann, 2000** Shappell, S.A., and Wiegmann, D.A., 2000, The human factors analysis and classification system (HFACS): US Department of Transportation Office of Aviation Medicine, 20 p., doi:10.4324/9781315263878-3.

[Google Scholar](#)

**Sharma and Van Gent, 2018** S. Sharma, D. Van Gent

The Australian South West hub project: developing confidence in migration assisted trapping in a saline aquifer – understanding uncertainty boundaries through scenarios

that stress the models

SSRN Electron. J. (2018), [10.2139/ssrn.3366170](https://ssrn.com/abstract=3366170) ↗

[Google Scholar](#) ↗

[Sharma et al., 2017](#) S. Sharma, D. Van Gent, M. Burke, L. Stelfox

The Australian South West Hub Project: developing a storage project in unconventional geology

Energy Procedia, 114 (2017), pp. 4524-4536, [10.1016/j.egypro.2017.03.1569](https://doi.org/10.1016/j.egypro.2017.03.1569) ↗

v

 [View PDF](#) [View article](#) [View in Scopus](#) ↗ [Google Scholar](#) ↗

[Snedden and Galloway, 2019](#) J.W. Snedden, W.E. Galloway

The gulf of Mexico sedimentary basin

Depositional Evolution and Petroleum Applications, Cambridge University Press (2019),

[10.1017/9781108292795](https://doi.org/10.1017/9781108292795) ↗

[Google Scholar](#) ↗

[Spencer and Collins, 2022](#) J. Spencer, L. Collins

Waterworld: How Ukraine Flooded Three Rivers to Help Save Kyiv

Modern War Institute (2022)

<https://mwi.usma.edu/waterworld-how-ukraine-flooded-three-rivers-to-help-save-kyiv/> ↗

accessed July 2022

[Google Scholar](#) ↗

[Sylta, 2002](#) Ø. Sylta

Quantifying secondary migration efficiencies: secondary migration efficiencies

Geofluids, 2 (2002), pp. 285-298, [10.1046/j.1468-8123.2002.00044.x](https://doi.org/10.1046/j.1468-8123.2002.00044.x) ↗

v

[View in Scopus](#) ↗ [Google Scholar](#) ↗

[Tanimoto et al., 2020](#) Tanimoto, S., Takahashi, Y., Takeishi, A., Wangyal, S., Dechen, T., Sato, H., and Kanai, A., 2020, Concept proposal of multi-layer defense security countermeasures based on dynamic reconfiguration multi-perimeter lines, in Barolli, L., Nishino, H., Enokido, T., and Takizawa, M. eds., Advances in Networked-Based Information Systems, Cham, Springer International Publishing, Advances in Intelligent Systems and Computing, v. 1036, p. 413–422, doi:10.1007/978-3-030-29029-0\_39.

[Google Scholar](#) ↗

[UIC Class VI 2010](#) UIC Class VI, 2010, Title 40 CFR Parts 124, 144, 145, 146 and 147: federal requirements under the underground injection control (UIC) program for carbon dioxide (CO<sub>2</sub>) geologic sequestration (GS) wells, <https://ecfr.io/cgi-bin/text-idx?SID=d6f7aaae2870c971ee751b8d4a6a90b4&mc=true&node=sp40.25.146.h&rgn=div6> ↗ (accessed July 2021).

[Google Scholar](#) ↗

[US EPA 2013](#) US EPA, 2013, Geologic sequestration of carbon dioxide: underground injection control (UIC) program class VI well testing and monitoring guidance.

[Google Scholar ↗](#)

[Verrien et al., 1967](#) J.P. Verrien, G. Courand, L. Montadert

Applications of production geology methods to reservoir characteristics analysis from outcrops observation

Proceedings of the 7th World Petroleum Congress, Mexico, SPE (1967), pp. 425-467

[View in Scopus ↗](#) [Google Scholar ↗](#)

[Vithanage et al., 2012](#) M. Vithanage, P. Engesgaard, K.H. Jensen, T.H. Illangasekare, J. Obeysekera

Laboratory investigations of the effects of geologic heterogeneity on groundwater salinization and flush-out times from a tsunami-like event

J. Contam. Hydrol., 136–137 (2012), pp. 10-24, [10.1016/j.jconhyd.2012.05.001 ↗](#)

v

 [View PDF](#) [View article](#) [View in Scopus ↗](#) [Google Scholar ↗](#)

[Wentworth, 1922](#) C.K. Wentworth

A scale of grade and class terms for clastic sediments

J. Geol., 30 (1922), pp. 377-392, [10.1086/622910 ↗](#)

v

[Google Scholar ↗](#)

[Williams and Chadwick, 2021](#) G.A. Williams, R.A. Chadwick

Influence of reservoir-scale heterogeneities on the growth, evolution and migration of a CO<sub>2</sub> plume at the Sleipner Field, Norwegian North Sea

Int. J. Greenh. Gas Control, 106 (2021), Article 103260, [10.1016/j.ijggc.2021.103260 ↗](#)

v

 [View PDF](#) [View article](#) [View in Scopus ↗](#) [Google Scholar ↗](#)

[Zeito, 1965](#) G.A. Zeito

Interbedding of shale breaks and reservoir heterogeneities

J. Pet. Technol., 17 (1965), pp. 1223-1228, [10.2118/1128-PA ↗](#)

v

[Google Scholar ↗](#)

[Zetaware 2022](#) Zetaware, 2022, ZetaWare source rock potential calculators,

<https://www.zetaware.com/utilities/srp/index.html> ↗ (accessed June 2022).

[Google Scholar ↗](#)

---

Cited by (2)

## [A Deep Learning-Based Workflow for Fast Prediction of 3d State Variables in Geological Carbon Storage: A Dimension Reduction Approach ↗](#)

2023, SSRN

## [Impact of Pressure-Dependent Interfacial Tension and Contact Angle on Capillary Trapping and Storage of CO<sub>2</sub> in Saline Aquifers ↗](#)

2023, Proceedings - SPE Annual Technical Conference and Exhibition

© 2023 The Author(s). Published by Elsevier Ltd.



All content on this site: Copyright © 2023 Elsevier B.V., its licensors, and contributors. All rights are reserved, including those for text and data mining, AI training, and similar technologies. For all open access content, the Creative Commons licensing terms apply.

